

基于MRI征象建立预测肝细胞癌相关恶病质的列线图

李信响¹ 刘兵² 江洋¹ 赵宇飞¹ 彭新桂^{1△}

(¹东南大学附属中大医院放射科 南京 210009; ²中国科学技术大学附属第一医院(安徽省立医院)影像科 合肥 230001)

【摘要】 目的 探讨治疗前MRI征象预测肝细胞癌(hepatocellular carcinoma, HCC)相关恶病质的价值。方法 回顾性分析399例HCC患者治疗前临床和MRI资料。所有患者均进行MRI平扫及增强检查,并随访MRI检查后6个月时患者的体重。根据恶病质诊断标准,将患者分为恶病质组和非恶病质组。按照随机抽样将所有病例分为训练集($n=279$)和验证集($n=120$)。利用单因素和多因素逻辑回归分析筛选与HCC相关恶病质的变量,建立预测模型。采用受试者工作特征(receiver operating characteristic, ROC)曲线评估不同模型的预测效能,采用DeLong检验比较不同模型AUC值,选择最佳性能模型建立预测HCC相关恶病质列线图。结果 多因素逻辑回归分析显示,血清白蛋白 <40 g/dL、血清甲胎蛋白 >100 ng/mL、肿瘤直径 >5 cm、门静脉癌栓、瘤内强化动脉和动脉期肿瘤边缘肝实质强化是预测肝细胞癌相关恶病质独立危险因素,临床-影像模型预测性能最好,训练集区分度AUC达0.843,验证集达0.854。结论 依据MRI征象建立列线图可较临床诊断提前6个月预测HCC相关恶病质,具有重要的临床治疗指导意义。

【关键词】 肝细胞癌(HCC); 恶病质; MRI征象; 列线图

【中图分类号】 R735.7, R445.2 **【文献标志码】** A **doi:** 10.3969/j.issn.1672-8467.2025.01.002

Development of a nomogram for predicting cachexia in hepatocellular carcinoma based on MRI features

LI Xin-xiang¹, LIU Bing², JIANG Yang¹, ZHAO Yu-fei¹, PENG Xin-gui^{1△}

(¹Department of Radiology, Zhongda Hospital, Southeast University, Nanjing 210009, Jiangsu Province, China;

²Department of Radiology, the First Affiliated Hospital (Anhui Provincial Hospital), University of Science and Technology of China, Hefei 230001, Anhui Province, China)

【Abstract】 **Objective** To investigate the value of pre-treatment MRI features in predicting cachexia in hepatocellular carcinoma (HCC). **Methods** A retrospective analysis was conducted on 399 patients with hepatocellular carcinoma, recording their pre-treatment clinical and MRI data. All patients underwent MRI plain and enhanced scan, and their weight was followed up 6 months after the MRI examination. According to the diagnostic criteria for cachexia, patients were divided into cachexia group and non-cachexia group. They were randomly divided into the training set ($n=279$) and the validation set ($n=120$). Univariable and multivariable logistic regression analyses were used to screen variables associated with cachexia in hepatocellular carcinoma and to establish a predictive model. The receiver operating characteristic (ROC) curve was used to evaluate the predictive performance of different models. The DeLong test was used to compare the AUC values of different models, and the best-performing model was used to establish a

国家自然科学基金面上项目(82272064);东南大学附属中大医院江苏省高水平医院结对帮扶建设项目(zdlyg08)

[△]Corresponding author E-mail: xingui2005peng@126.com

网络首发时间:2024-11-13 13:33:49 网络首发地址:https://link.cnki.net/urlid/31.1885.R.20241112.1425.006

predictive nomogram for cachexia in hepatocellular carcinoma. **Results** Multivariable logistic regression analysis showed that serum albumin <40 g/dL, serum alpha-fetoprotein >100 ng/mL, tumor diameter >5 cm, portal vein tumor thrombus, intratumoral arterial enhancement, and arterial phase peritumoral enhancement were independent predictors of cachexia in hepatocellular carcinoma. The clinical-imaging model showed the best predictive performance, with an AUC of 0.843 in the training set and 0.854 in the validation set. **Conclusion** The nomogram based on MRI features can predict cachexia in hepatocellular carcinoma 6 months earlier than clinical diagnosis, which has important clinical guidance significance.

【Key words】 hepatocellular carcinoma (HCC); cachexia; MRI feature; nomogram

* This work was supported by the General Program of National Natural Science Foundation of China (82272064) and High-level Hospital Paring Assistance Construction Program of Zhongda Hospital affiliated to Southeast University, Jiangsu Province (zdlyg08).

肝细胞癌(hepatocellular carcinoma, HCC)是常见的恶性肿瘤之一,在我国居民肿瘤相关死因中列于第二位^[1]。恶病质是HCC预后差的重要独立危险因素^[2]。50.1%的HCC患者出现恶病质^[3]。癌症相关恶病质是肿瘤部位分泌相关代谢物导致骨骼肌和脂肪组织分解^[4]。癌症相关恶病质患者的化疗反应差、生活质量降低和预后差^[5]。恶病质的诊断标准^[6]是无节食下患者6个月内体重减轻超过5%或BMI低于 20 kg/m^2 且体重减轻超过2%,即恶病质的诊断需要随访6个月体重,故亟需一种早期诊断恶病质的方法。

HCC的MRI征象可预测微血管浸润、粗梁实体型肝细胞癌等多个恶性特征^[7-8]。以往的相关文献主要基于MRI骨骼肌面积减少、肌肉质量下降和质子密度脂肪分数来评估恶病质^[9-10],但需要相应软件进行测量。本研究通过治疗前HCC肿瘤部位的MRI征象预测恶病质,临床上易于操作,可早期识别有肝细胞癌相关恶病质发生风险的患者。

资料和方法

研究对象及分组 回顾性分析中国科学技术大学附属第一医院2015年5月至2021年6月期间接受MRI平扫及增强的HCC患者的临床资料。本研究由中国科学技术大学附属第一医院伦理委员会批准(批准号:2021-RE-091)。HCC的诊断基于2018年美国肝病研究协会诊断标准^[11]。纳入标准:(1)MRI扫描与HCC治疗间隔时间 ≤ 2 周;(2)患者至少有2次体重记录(MRI扫描至6个月随访期间)。排除标准:(1)MRI扫描时已接受HCC治疗的患者;(2)可能对体重有影响的合并症,如其

他肿瘤、胰腺炎、心力衰竭、肾病、慢性阻塞性肺病、急性胆囊炎、严重肝硬化、严重脂肪肝和大量腹水;(3)MRI扫描前30天体重变化较大患者;(4)图像质量不佳。再按照恶病质诊断标准,最终纳入研究患者399例。应用SPSS软件(26.0版本)按7:3简单随机抽样分为训练集($n=279$)和验证集($n=120$)(图1)。

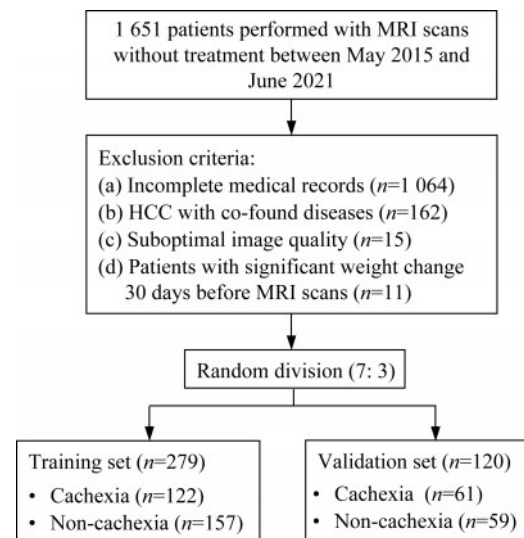


图1 患者筛选流程图

Fig 1 The flowchart used in selection of the patients

MRI扫描参数 采用西门子 TrioTim 3.0T MR扫描仪,八通道相控阵线圈,扫描范围为膈顶到肝脏下缘水平。MRI的同反向位T1WI为双回波梯度回波序列:TR 193 ms, TE 1.55 ms和3.06 ms, FOV $38 \text{ cm} \times 33.2 \text{ cm}$,层厚6.0 mm。FSE-T2WI参数:TR 1000 ms, TE 98 ms, FOV $39 \text{ cm} \times 26.8 \text{ cm}$,层厚6.0 mm。蒙片及多期增强采用3D GRE T1WI序列:TR 4.07 ms, TE 1.86 ms, FOV $38 \text{ cm} \times 30.9 \text{ cm}$,层厚2.5 cm,层间距0 mm,反转角 9° ;DWI

序列:TR 5111 ms,TE 73 ms,FOV 38 cm×28.5 cm,层厚 5.0 mm。所用造影剂包括 Gd-DTPA(剂量 0.2 mL/kg,流率 2.0 mL/s)和 Gd-EOB-DTPA(剂量 0.1 mL/kg,流率 2.0 mL/s),注射后用 20 mL 生理盐水进行稀释。注射对比剂后获取动脉期(20~25 s)、门静脉期(60~75 s)和延迟期(90~105 s),或肝胆期(20 min)的影像数据。

MRI 征象分析 MRI 征象由两名影像科医生进行双盲法阅片,意见不一致时,则协商达成一致。共 16 种征象。(1)肿瘤直径:T2WI 横轴位最大径,并对照增强序列进行测量;(2)多灶性:肿瘤数量≥2;(3)瘤内出血:T1WI 同相位上高信号,反相位信号未衰减;(4)瘤内脂肪:同相位高信号,反相位呈低信号;(5)肿瘤包膜:门静脉期、延迟期或过渡期肿瘤部分或全部周缘呈平滑、均匀及尖锐样强化;(6)肝脏包膜皱缩征:HCC 导致正常凸面肝脏轮廓内陷或局灶变平;(7)不规则肿瘤边界:肿瘤与周围正常肝组织之间的界限或界面为不规则或模糊的;(8)“结中结”征象:较大的结节内含小结节,且两者信号不同;(9)马赛克征:病灶内形状、大小不一致散在结节和分隔;(10)门静脉癌栓:T2WI 上和 T1 增强上门静脉内与肿瘤信号相一致信号;(11)瘤内强化动脉:动脉期可见散在强化动脉;(12)动脉期非环状高强度:动脉期整个病灶或一部分强化,高

于肝实质;(13)动脉期肿瘤周边肝实质强化:动脉期肿瘤边缘肝实质片状或半月形强化;(14)非周边廓清:肿瘤部分或全部较周围肝实质强化程度减低;(15)肝外转移:肝脏之外的肝癌转移灶;(16)弥散受限:肿瘤在 DWI 上信号强度高于肝实质,在 ADC 图上信号低于肝实质。

统计学分析 采用 SPSS 26.0 和 R 4.2.2 软件进行统计学分析,连续性数据采用中位数(四分位间距)表示,分类数据用百分比表示。单因素和多因素 Logistic 回归分析筛选与肝细胞癌相关恶病质相关的变量,单因素中 $P < 0.05$ 的变量纳入多因素回归分析中,经向后逐步回归法筛选最终变量。构建临床模型、影像模型和临床-影像模型。采用受试者工作特征(receiver operating characteristic curve, ROC)曲线和校准曲线图评估模型的性能,采用 DeLong 检验比较不同预测模型曲线下面积(area under the curve, AUC)的差异,选择性能最佳模型构建列线图。 $P < 0.05$ 为差异有统计学意义。

结 果

患者临床和 MRI 基线资料 训练集和验证集患者治疗前临床和 MRI 征象资料见表 1。两个数据集间性别存在统计学差异,余基线资料无统计学差异。

表 1 训练集和验证集的临床和 MRI 征象基线资料

Tab 1 Baseline clinical and MRI features of the training set and the validation set [M(P_{25} , P_{75}) or n(%)]

Features	Training set (n=279)	Validation set (n=120)	P	Statistical value
Clinical characteristics				
Age (y)	55.0 (49.0,65.0)	54.0 (49.0,64.0)	0.40	Z=-0.85
Sex (males: females)	244:35	90:30	<0.01	$\chi^2=9.55$
BMI (kg/m ²)	23.4 (21.5,25.7)	23.7 (21.8,25.6)	0.23	Z=-1.21
Aspartate transaminase (IU/L)	44.0 (30.0,61.0)	46.0 (31.0,62.8)	0.62	Z=-0.50
Alanine transaminase (IU/L)	38.0 (26.0,58.0)	37.0 (26.0,55.4)	0.63	Z=-0.48
Albumin (g/L)	39.9 (36.6,42.8)	39.5 (36.2,42.9)	0.32	Z=-1.00
Bilirubin (mg/dL)	17.3 (12.5,23.9)	17.2 (12.6,23.9)	0.98	Z=-0.02
α -fetoprotein (ng/mL)	73.0 (10.1,536.4)	116.5 (16.5,838.7)	0.14	Z=-1.48
MRI features				
Tumor size (cm)	4.9 (3.3,8.3)	5.1 (2.8,9.2)	0.97	Z=-0.04
Multifocality	120 (43.0)	51 (42.5)	0.93	$\chi^2=0.01$
Blood products in mass	106 (38.0)	45 (37.5)	0.93	$\chi^2=0.01$
Intralesional fat	46 (16.5)	15 (12.5)	0.36	$\chi^2=1.03$
Tumor capsule			0.91	$\chi^2=0.20$
Complete	110 (39.4)	48 (40.0)		
Incomplete	122 (43.7)	50 (41.7)		

(续表 1)

Features	Training set (n=279)	Validation set (n=120)	P	Statistical value
None	47 (16.8)	22 (18.3)		
Hepatic capsular retraction	123 (44.1)	51 (42.5)	0.77	$\chi^2=0.09$
Ill-defined tumor margin	162 (58.1)	69 (57.5)	0.92	$\chi^2=0.01$
Nodule-in-nodule	60 (21.5)	34 (28.3)	0.14	$\chi^2=2.12$
Mosaic architecture	141 (50.5)	66 (55.0)	0.41	$\chi^2=0.67$
Portal vein tumor thrombus	68 (24.4)	32 (26.7)	0.63	$\chi^2=0.24$
Intratumoral artery	136 (48.7)	64 (53.3)	0.40	$\chi^2=0.71$
Nonrim arterial phase hyperenhancement	211 (75.6)	95 (79.2)	0.44	$\chi^2=0.59$
Arterial phase peritumoral enhancement	131 (47.0)	53 (44.2)	0.61	$\chi^2=0.26$
Nonperipheral washout	262 (93.9)	114 (95.0)	0.67	$\chi^2=0.67$
Extrahepatic metastasis	33 (11.8)	11 (9.2)	0.44	$\chi^2=0.61$
Restricted diffusion	215 (77.1)	85 (70.8)	0.21	$\chi^2=1.74$

单因素和多因素逻辑回归分析筛选与肝细胞癌恶病质相关的变量。经单因素和多因素逻辑回归分析发现,血清白蛋白 <40 g/L (OR: 3.51; 95%CI: 1.90~6.49; $P<0.01$)、AFP >100 ng/mL (OR: 2.54; 95% CI: 1.40~4.61; $P<0.01$)、肿瘤直径 >5 cm (OR: 2.14; 95% CI: 1.07~4.26; $P=$

0.03)、门静脉癌栓(OR: 2.55; 95%CI: 1.24~5.26; $P=0.01$)、瘤内强化动脉(OR: 2.23; 95%CI: 1.10~4.52; $P=0.03$)和动脉期肿瘤边缘肝实质强化(OR: 2.58; 95%CI: 1.34~4.98; $P<0.01$)是肝细胞癌相关恶病质发生的独立危险因素(表2)。

表2 单因素和多因素逻辑回归分析筛选与肝细胞癌相关恶病质相关的变量

Tab 2 Univariable and multivariable analyses screen variables associated with cachexia in HCC

Clinical and imaging features	Univariable analysis		Multivariable analysis	
	Odds ratio (95%CI)	P	Odds ratio (95% CI)	P
Albumin <40 g/L	2.65 (1.62-4.31)	<0.01	3.51 (1.90-6.49)	<0.01
Aspartate transaminase >45 IU/L	1.61 (1.00-2.60)	<0.05	0.70 (0.38-1.32)	0.27
α -fetoprotein >100 ng/mL	3.42 (2.08-5.61)	<0.01	2.54 (1.40-4.61)	<0.01
Tumor size >5 cm	6.12 (3.63-10.35)	<0.01	2.14 (1.07-4.26)	0.03
Multifocality	1.87 (1.16-3.03)	0.01	1.26 (0.68-2.32)	0.46
Hepatic capsular retraction	1.83 (1.13-2.96)	0.01	0.73 (0.37-1.42)	0.35
Ill-defined tumor margin	2.24 (1.37-3.67)	<0.01	0.96 (0.48-1.92)	0.91
Portal vein tumor thrombus	5.92 (3.19-10.98)	<0.01	2.55 (1.24-5.26)	0.01
Intratumoral artery	5.88 (3.49-9.90)	<0.01	2.23 (1.10-4.52)	0.03
Arterial phase peritumoral enhancement	5.95 (3.53-10.01)	<0.01	2.58 (1.34-4.98)	<0.01
Extrahepatic metastasis	2.92 (1.36-6.29)	<0.01	1.62 (0.61-4.28)	0.34

预测肝细胞癌相关恶病质列线图的建立和验证。ROC分析得出,在训练集中,临床模型、影像模型和临床-影像模型的AUC值为0.712、0.792和0.843(表3和图2)。在验证集中,临床模型、影像模型和临床-影像模型的AUC值为0.749、0.772和0.854。DeLong检验比较得出,在两个数据集中,临床-影像模型与临床模型、临床-影像模型与影像模型AUC比较均有统计学意义(P 均 <0.05)。在校准曲线分析中,采用自助抽样法重复采样1 000次,

训练集和验证集中,临床-影像模型预测肝细胞癌相关恶病质发生风险与实际发生风险的一致性良好,平均绝对误差均为0.03,接近0(图3)。综上所述,临床-影像模型在训练集和验证集中性能均最佳,故选择临床-影像模型建立列线图(图4)。列线图预测肝细胞癌相关恶病质的病例见图5和6。这两个病例提示本研究所筛选的MRI征象和实验室指标建立的列线图在预测肝细胞癌相关恶病质上是可行的。

表3 训练集、内部验证集和外部验证集中三个模型预测肝细胞癌相关恶病质的性能

Tab 3 The performance of the 3 models predicting cachexia in HCC in the training set and internal/external validation set

Cohorts	Models	Sensitivity	Specificity	AUC (95%CI)	P
Training set	Clinical model	0.918	0.420	0.712 (0.654–0.770)	<0.01*
	Imaging model	0.631	0.866	0.792 (0.737–0.846)	<0.01 [#]
	Clinical-imaging model	0.762	0.796	0.843 (0.797–0.889)	
Validation set	Clinical model	0.705	0.695	0.749 (0.665–0.833)	<0.01*
	Imaging model	0.803	0.627	0.772 (0.690–0.854)	<0.01 [#]
	Clinical-imaging model	0.738	0.831	0.854 (0.788–0.920)	

* Clinical model vs. clinical-imaging model. [#] Imaging model vs. clinical-imaging model.

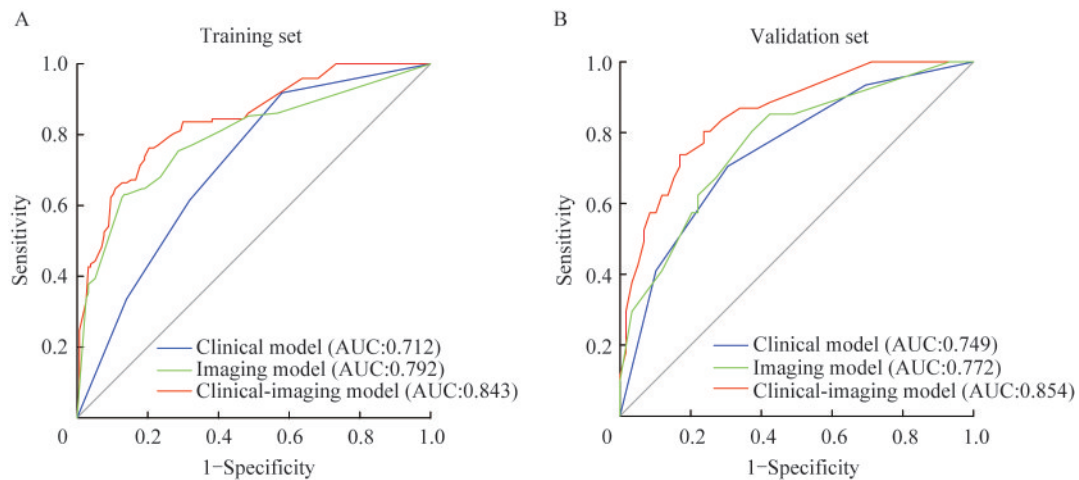


图2 训练集(A)和验证集(B)中临床模型、影像模型和临床-影像模型的ROC分析

Fig 2 ROC analysis of clinical model, imaging model, and clinical-imaging model in the training set (A) and validation set (B)

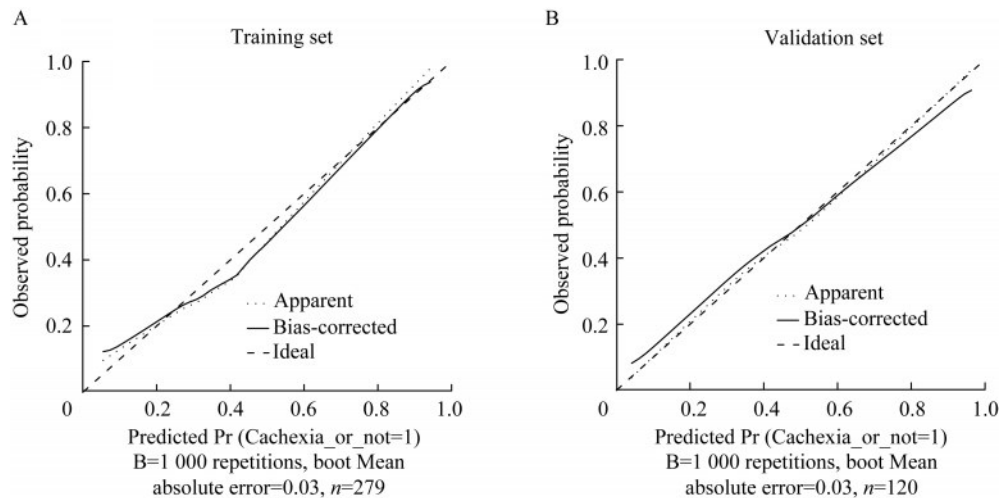


图3 训练集和验证集的临床-影像模型预测肝细胞癌相关恶病质的校准曲线图

Fig 3 Calibration curve of the clinical-imaging model predicting cachexia in hepatocellular carcinoma in the training set and validation set

讨 论

癌症相关恶病质是由癌症本身产生的代谢物

引起骨骼肌和脂肪组织的丢失,导致患者预后不良且对治疗反应较差。临床上对癌症患者多注重原发灶的治疗而忽视癌症相关恶病质的治疗,恶病质进一步发展会转为恶病质难治期,此时患者对抗癌

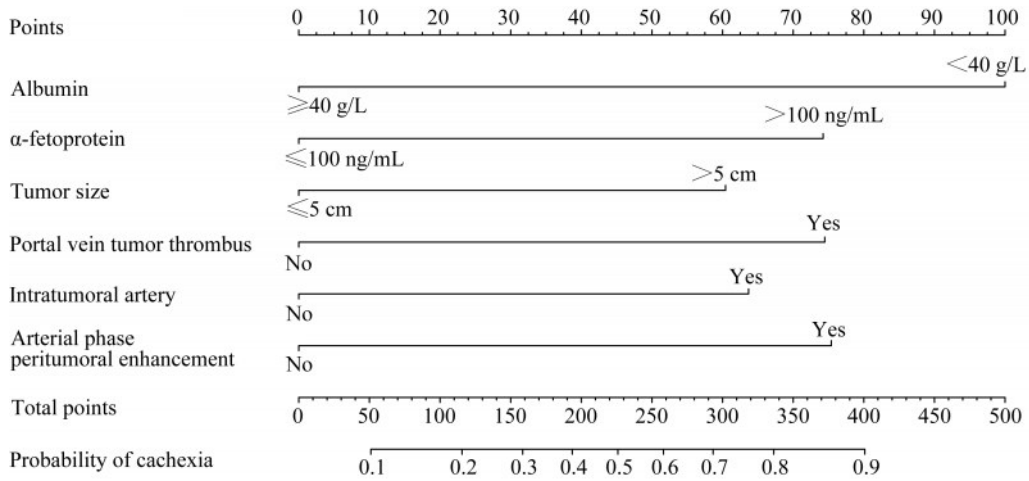
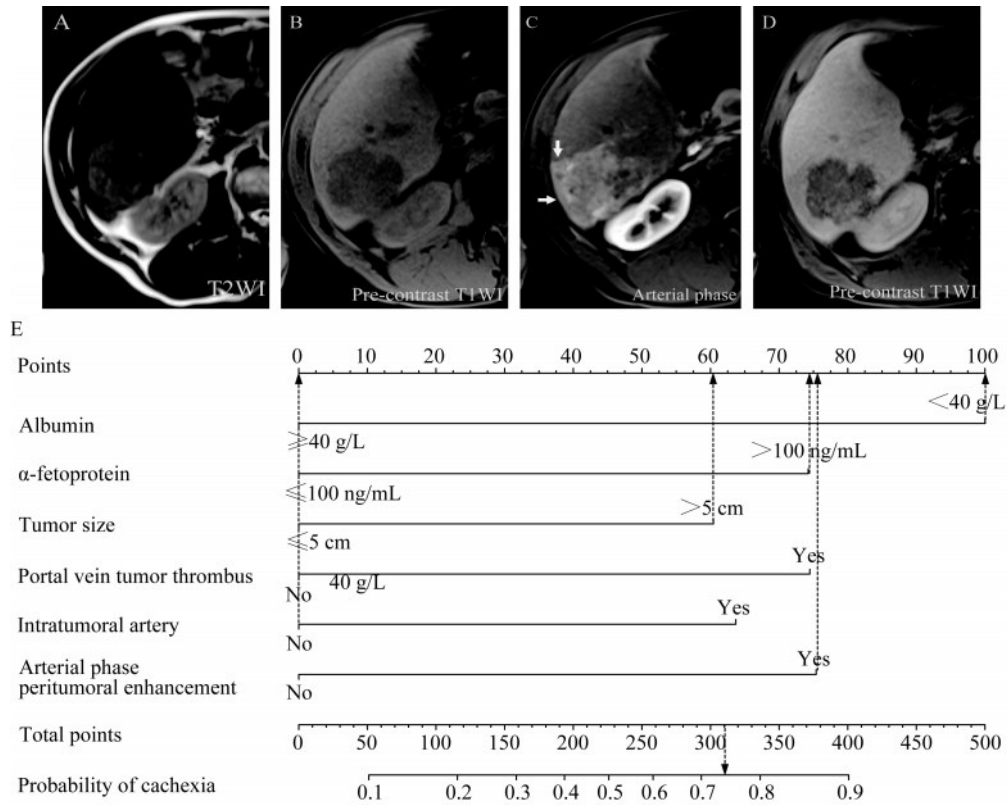


图4 基于临床-影像模型构建列线图

Fig 4 Nomogram constructed based on the clinical-imaging model



The patient underwent surgical resection after MRI scanning. Diagnosed with cachexia after a 5-month follow-up, the serum albumin of this patient was 38.3 g/L and α -fetoprotein was 1 210 ng/mL. A 6.0 cm mass was observed in the right lobe of the liver, showing moderate high signal on T2-weighted image (A), low signal on T1-weighted image with fat suppression (B), peritumoral enhancement on the arterial phase (C, white arrow), and the tumor appeared as a low signal on the delayed phase (D). E: The total score of the nomogram for this case was $100+74+61+0+0+75.5=310.5$, corresponding to a predicted probability of 74% for cachexia.

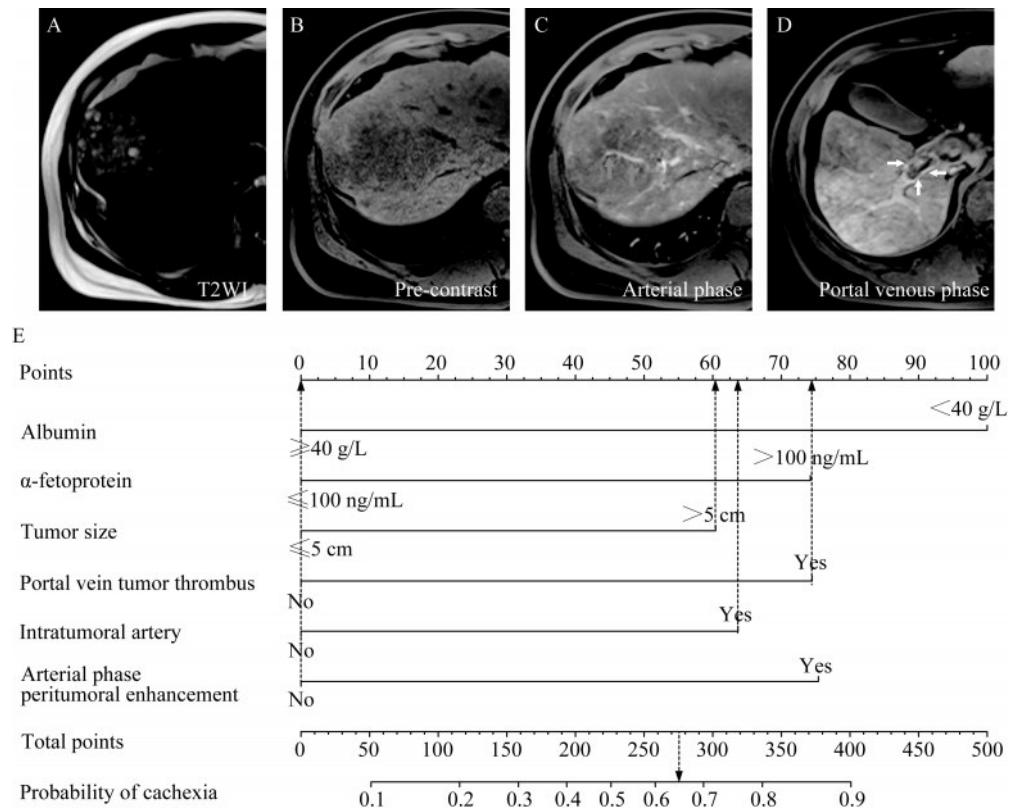
图5 1例52岁男性HCC相关恶病质MRI图

Fig 5 MRI of a 52-year-old man with hepatocellular carcinoma associated cachexia

治疗无反应,且预期寿命少于3个月,因此及时对恶病质进行干预十分重要^[6]。

本研究开发并验证了一种基于血清学检查和

肿瘤本身的MRI征象预测肝细胞癌相关恶病质的列线图,以早期判别可能发生恶病质风险的患者,并进行提前干预。该列线图包含的独立危险因素有血清



The patient underwent transarterial chemoembolization after MRI scanning. Diagnosed with cachexia after a 2-month follow-up, his serum albumin was 53.1 g/L and α -fetoprotein was 379.3 ng/mL. A 7.7 cm mass was observed in the right lobe of the liver, showing moderate high signal on T2-weighted image (A), low signal on pre-contrast T1-weighted image (B), intratumoral artery on the arterial phase (C), blue arrow), and portal vein tumor thrombus on the portal venous phase (D, white arrow). E: The total score of the nomogram for this case was $0+74+61+74+63.5+0=272.5$, corresponding to a predicted probability of 64% for cachexia.

图6 1例35岁男性HCC相关恶病质MRI图

Fig 6 MRI of a 35-year-old man with HCC associated cachexia

白蛋白<40 g/dL、血清甲胎蛋白>100 ng/mL、肿瘤直径>5 cm、门静脉癌栓、瘤内强化动脉和动脉期肿瘤边缘肝实质强化,其预测性能较好,训练集区分度达0.843、验证集达0.854。

据文献报道^[12],恶病质患者的血清白蛋白低于非恶病质,与本研究结果一致。其原因可能是低血清白蛋白时,骨骼肌蛋白的合成和分解的平衡受到破坏,进而骨骼肌质量下降。此外,本研究中血清甲胎蛋白>100 ng/mL与HCC相关恶病质发生独立相关,与文献报道一致^[13]。文献表明,高水平的血清甲胎蛋白与HCC微血管浸润、增殖型肝细胞癌、差的预后等不良结果相关^[14-16],这些恶性特征更可能发生恶病质。这可能是本研究中高血清甲胎蛋白水平是恶病质独立危险因素的原因。在MRI征象的分析中,肿瘤直径>5 cm与HCC相关恶病质独立相关,与已发表的文献报道相一致^[2]。肿瘤

越大,其分期可能越处于晚期,且其分泌肿瘤代谢物可能更多。同时,肿瘤晚期患者更易发生恶病质^[4],骨骼肌损失通常发生在肿瘤较大的HCC患者^[17]。所以肿瘤直径越大越可能发生恶病质。HCC患者发生门静脉癌栓时,按照巴塞罗那HCC分期处于晚期,故易发生恶病质。MRI征象的瘤内强化动脉和动脉期肿瘤边缘肝实质强化是HCC的恶性征象,据文献报道^[7-8],其可以预测HCC的微血管浸润、粗梁实体型HCC等不良结果,同时这两种征象的HCC预后也差,发生恶病质的可能性也越大。

本研究不足之处:首先,作为回顾性研究,在病例收集时筛除了随访中无体重记录的患者,可能产生偏倚;其次,研究中患者饮食情况病历中无记录,是否对研究有影响需要进一步研究验证。

综上所述,本研究中建立的多变量列线图可预

测HCC相关恶病质,可比临床诊断提前6个月,且无需对患者的体重进行随访,对HCC患者的临床治疗决策有重要的指导意义。

作者贡献声明 李信响 数据采集,统计分析,论文撰写和修订。刘兵,江洋,赵宇飞 数据采集,研究设计,论文修订。彭新桂 研究设计,论文修订,获取资助,监督指导。

利益冲突声明 所有作者均声明不存在利益冲突。

参 考 文 献

- [1] QI J, LI M, WANG L, *et al.* National and subnational trends in cancer burden in China, 2005-20: an analysis of national mortality surveillance data [J]. *The Lancet Public Health*, 2023, 8(12): e943-e955.
- [2] RICH NE, PHEN S, DESAI N, *et al.* Cachexia is prevalent in patients with hepatocellular carcinoma and associated with worse prognosis [J]. *Clin Gastroenterol Hepatol*, 2022, 20(5): e1157-e1169.
- [3] ANKER MS, HOLCOMB R, MUSCARITOLI M, *et al.* Orphan disease status of cancer cachexia in the USA and in the European Union: a systematic review [J]. *J Cachexia Sarcopenia Muscle*, 2019, 10(1): 22-34.
- [4] BARACOS VE, MARTIN L, KORC M, *et al.* Cancer-associated cachexia [J]. *Nat Rev Dis Primers*, 2018, 4: 17105.
- [5] MORIMOTO K, UCHINO J, YOKOI T, *et al.* Impact of cancer cachexia on the therapeutic outcome of combined chemoimmunotherapy in patients with non-small cell lung cancer: a retrospective study [J]. *Oncoimmunology*, 2021, 10(1): 1950411.
- [6] FEARON K, STRASSER F, ANKER SD, *et al.* Definition and classification of cancer cachexia: an international consensus [J]. *Lancet Oncol*, 2011, 12(5): 489-495.
- [7] LEE S, KIM SH, LEE JE, *et al.* Preoperative gadoxetic acid-enhanced MRI for predicting microvascular invasion in patients with single hepatocellular carcinoma [J]. *J Hepatol*, 2017, 67(3): 526-534.
- [8] RHEE H, CHO ES, NAHM JH, *et al.* Gadoteric acid-enhanced MRI of macrotrabecular-massive hepatocellular carcinoma and its prognostic implications [J]. *J Hepatol*, 2021, 74(1): 109-121.
- [9] HAN J, HARRISON L, PATZELT L, *et al.* Imaging modalities for diagnosis and monitoring of cancer cachexia [J]. *EJNMMI Res*, 2021, 11(1): 94.
- [10] PATZELT L, JUNKER D, SYVÄRI J, *et al.* MRI-determined psoas muscle fat infiltration correlates with severity of weight loss during cancer cachexia [J]. *Cancers (Basel)*, 2021, 13(17): 4433.
- [11] HEIMBACH JK, KULIK LM, FINN RS, *et al.* AASLD guidelines for the treatment of hepatocellular carcinoma [J]. *Hepatology*, 2018, 67(1): 358-380.
- [12] BLUM D, STENE GB, SOLHEIM TS, *et al.* Validation of the consensus-definition for cancer cachexia and evaluation of a classification model--a study based on data from an international multicentre project (EPCRC-CSA) [J]. *Ann Oncol*, 2014, 25(8): 1635-1642.
- [13] YANG QJ, ZHAO JR, HAO J, *et al.* Serum and urine metabolomics study reveals a distinct diagnostic model for cancer cachexia [J]. *J Cachexia Sarcopenia Muscle*, 2018, 9(1): 71-85.
- [14] ENDO Y, ALAIMO L, LIMA HA, *et al.* A novel online calculator to predict risk of microvascular invasion in the preoperative setting for hepatocellular carcinoma patients undergoing curative-intent surgery [J]. *Ann Surg Oncol*, 2023, 30(2): 725-733.
- [15] KANG HJ, KIM H, LEE DH, *et al.* Gadoteric acid-enhanced MRI features of proliferative hepatocellular carcinoma are prognostic after surgery [J]. *Radiology*, 2021, 300(3): 572-582.
- [16] LIN K, HUANG Q, ZENG J, *et al.* Clinical significance of alpha-fetoprotein in alpha-fetoprotein negative hepatocellular carcinoma underwent curative resection [J]. *Dig Dis Sci*, 2021, 66(12): 4545-4556.
- [17] IMAI K, TAKAI K, MIWA T, *et al.* Rapid depletions of subcutaneous fat mass and skeletal muscle mass predict worse survival in patients with hepatocellular carcinoma treated with Sorafenib [J]. *Cancers (Basel)*, 2019, 11(8): 1206.

(收稿日期:2024-04-02; 编辑:张秀峰)